Contrib. Plasma Phys. **43**, No. 2, 111 – 121 (2003) / **DOI** 10.1002/ctpp.200310012

Effects of electron-absorbing boundaries on the plasma parameters of a hot-filament discharge

N. Jelić[*] [1], **R. Schrittwieser** [2], and **S. Kuhn** [3]

[1] Faculty of Mechanical Engineering, University of Ljubljana, Askerceva 6, SI-1000 Ljubljana, Slovenia
[2] Department of Ion Physics, University of Innsbruck, Technikerstrasse 25, A-6020 Innsbruck, Austria
[3] Department of Theoretical Physics, University of Innsbruck, Technikerstrasse 25, A-6020 Innsbruck, Austria

Received 4 October 2002, revised 27 January 2003, accepted 20 February 2003
Published online 6 May 2003

Key words Hot-filament discharges, double-plasma devices, electrodes, probes, plasma-sheath, plasma layers.
PACS 52.75.Xx

In this paper we investigate theoretically and experimentally the plasma parameters in a double-plasma device in the presence of an additional electron-absorbing boundary. The latter is formed by an electrode of variable size immersed in the plasma. It is found that, depending on its size and bias potential, such an anode can considerably influence the plasma parameters. Good qualitative and fair quantitative agreement between theoretical predictions and laboratory measurements of the plasma parameters is found for various discharge conditions. In addition we discuss the consequences of our results with respect to the existence conditions of anode-type double layers in double-plasma devices.

1 Introduction

The question of whether and how an electron-absorbing boundary can influence the plasma parameters of a hot-filament discharge is of interest in many laboratory experiments. Experimentally, such an electron-absorbing boundary may be realized in different ways. For instance, questions may arise concerning the perturbation of plasma parameters induced by probe measurements (e.g. [1]). Or, one might be interested in the global behaviour of plasma parameters in the presence of large objects, such as positively biased wire grids and anodes. It has been shown that a positively biased wire grid can serve either to control the plasma potential [2], or to raise the electron temperature [3]. Large probes and anodes were used for driving the plasma potential [4] and for producing anode-type double layers [5, 6, 7].

The present investigation differs from the previous ones in several features. First, we are interested in the effects of an electron-absorbing surface of variable size, rather than considering just a special electrode surface area. This approach enables us to give an *explicit* definition of what are "small" and "large" electron-absorbing boundaries. Second, we investigate a complete set of parametric dependencies of the plasma parameters on given external conditions, i.e., the plasma potential, the ion and electron densities, and the electron temperature as functions of external parameters such as anode size and bias potential, gas pressure and type, etc. Due to the high number of possible external-parameter combinations, this latter task appears to be extremely difficult unless we find out how to reduce the number of necessary measurements *in advance* and how to present the experimental data in an economic way. For that purpose we develop a model based on the simple theory of hot-filament discharges presented in the related paper [8], which we shall herefrom refer to as "similarity rules". According to the latter, the plasma parameters depend on a well-defined combination of the external parameters named the *discharge efficiency*, rather than on each of these parameters independently.

In addition, we identify the most elementary conditions that must be fulfilled in order to achieve (or prevent) formation of an anode-type double layer by means of a positively biased electrode (e.g., a large plane probe). It

[*] Corresponding author: e-mail: nikola.jelic@uibk.ac.at or: jelic@3d-ta.si

 0863-1042/03/0205-0111 $ 17.50+.50/0

appears that at present even the most elementary questions concerning the appearance of anode-type double layers under rather simple laboratory conditions are still far from being understood. Investigations on such double layers in double-plasma (DP) devices were always performed with anodes whose areas had to be chosen empirically on the basis of a trial-and-error procedure. However, it turns out that particular observations made in a particular DP device cannot simply be extended to other DP devices. An anode of given size, which was found quite suitable for obtaining and investigating anode-type double layers, e.g., at the University of Iowa [7] may appear entirely inappropriate for the University of Innsbruck DP Machine (present work).

Furthermore, the previous attempts aimed at the *theoretical* modeling of double layers always involved the assumption of *given* plasma parameters on both sides of the double layer. As will be seen here, the validity of this assumption may be seriously questioned since in the presence of a double layer the plasma parameters usually depend strongly on each other and can hardly be experimentally and theoretically decoupled. The purpose of the present investigation is to make a step toward (i) predicting the behavior of the plasma parameters in the presence of a positively biased anode or an anode-type double layer, and (ii) finding an optimum experimental set-up and giving an appropriate advance prescription for data acquisition and presentation, rather than laboriously extracting experimental results a posteriori.

In the next section we develop the theoretical model and present the related considerations. In Sec. 3 the theoretical results are applied to different noble gases at a fixed pressure, and to argon at different pressures. In Sec. 4 experimental results are given for varying external parameters. The particular consequences of these results are briefly discussed in Sec. 5 and our experimental and theoretical results are summarized in Sec. 6.

2 Theoretical model

An idealized hot-filament discharge with an additional electron-absorbing boundary (biased electrode or an anode-type double layer) is presented schematically in Fig. 1. The plasma, being in contact with a wall of

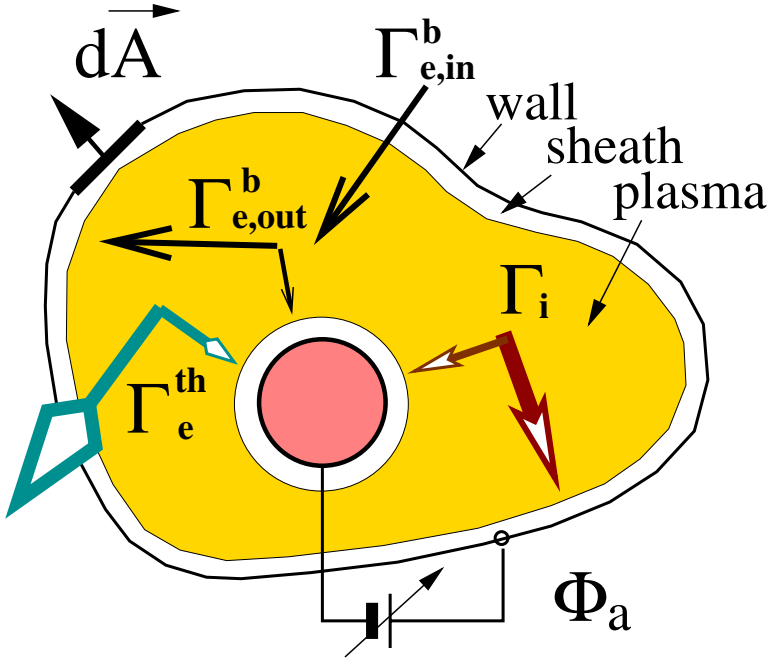

Fig. 1 (online colour at: www.interscience.wiley.com) An idealized discharge maintained by an external electron beam, with an additional electron-absorbing boundary.

area A_w whose geometry is arbitrary in principle, is maintained in a stationary state. The external energy source for plasma production is provided by a beam of primary electrons with energy $e\Phi^b$, which may be emitted either from a hot cathode or from another plasma of surface area $A^b_{e,in}$. Due to volume scattering processes and reflection at magnetic cusps (if present), these electrons usually spread quickly in phase space and finally get lost at

the total effective surface of area $A^b_{e,out}$. An additional electrode (anode) with surface area A_a is immersed in the plasma at an arbitrary position and biased at a potential Φ_a positive with respect to the wall.

In particular plasma experiment both the wall and the electrode can be replaced with other physical surfaces of interest, such as double layers, with no essential consequences for the present considerations.

The plasma parameters (i.e., the plasma potential Φ as measured with respect to the wall, the bulk-electron and ion densities n_e^{th} and n_i, respectively, and the bulk-electron temperature T_e) have to be calculated under the condition that the particle losses to the wall outweigh the volume losses. The main external parameters are the ratio $a_a = A_a/A$ of the anode surface to the total surface $A = A_a + A_w$, the total electron-beam input current $I^b_{e,in}$, the beam energy $e\Phi^b(\gg e\Phi)$, and the neutral-gas type and pressure. Here we shall assume that there are magnetic cusp lines uniformly distributed over the wall surface, but the main features of the model do not change essentially if the wall is replaced with another plasma at zero boundary potential. Our reference situation, however, corresponds to a single-plasma device with hot filaments in which there is either a positively biased electrode (i.e., probe) or a localized anode-type double layer.

In order to establish a mathematical model of our idealized plasma discharge, we use the basic equations presented in [8]. We consider two electron populations, the first one originating from the external beam electrons reflected at the magnetic cusps or scattered by some unspecified volume mechanism. In the vicinity of these electron emitter, the velocity distribution of the beam electrons can be modeled by a one-dimensional Dirac δ-function. However, in the plasma body the beam electrons are almost isotropically distributed in velocity space [9] and, consequently, can be represented by a velocity-in-shell distribution f^b_e. The second population is assumed to consist of Maxwellian-distributed bulk electrons (f^{th}_e). The ions are born at rest, acquiring their kinetic energy due to the self-consistently generated plasma potential profile which tends to confine the electrons and to enhance the ion removal from the plasma. The appropriate particle, charge and energy balance equations, which hold provided the electric field may be neglected (i.e., in the quasineutral plasma region [8]), are

$$\oint_A \mathbf{\Gamma}^b_e \cdot d\mathbf{A} = -\int_V \gamma^b_I dV, \tag{1}$$

$$\oint_A \mathbf{\Gamma}_i \cdot d\mathbf{A} = \int_V \gamma_I dV, \tag{2}$$

$$\oint_A \mathbf{J} \cdot d\mathbf{A} = 0, \tag{3}$$

and

$$\oint_A (\mathbf{Q}^{th}_e + \mathbf{Q}_i) \cdot d\mathbf{A} = -\oint_A \mathbf{Q}^b_e \cdot d\mathbf{A} - e\Phi_I \oint_V \mathbf{\Gamma}_i \cdot d\mathbf{A}, \tag{4}$$

where V is the plasma volume, bounded by the total plasma-sheath boundary A which is assumed to be approximately an equipotential surface. The particle- and energy-flux densities are defined by $\mathbf{\Gamma}_{e,i} = \int_{\mathbf{v}} f_{e,i}(\mathbf{v})\mathbf{v}d^3\mathbf{v}$ and $\mathbf{Q}_{e,i} = \frac{1}{2}m_{e,i}\int_{\mathbf{v}} f_{e,i}(\mathbf{v})v^2\mathbf{v}d^3\mathbf{v}$, respectively, $\mathbf{J}$ is the electric current density, $\gamma^{b,th}_I = \int n_a\sigma_I(v)v f^{b,th}_e(v)d^3\mathbf{v}$ are the partial ionization rates due to beam- and thermal-electron collisions with the working-gas atoms, respectively, $\gamma_I = \gamma^b_I + \gamma^{th}_I$ is the total ionization rate, Φ_I is the ionization potential, and n_a and σ_I are the gas density and the ionization cross-section, respectively.

With these definitions, the particle and energy flux densities for the beam electrons, the Maxwellian electrons and the cold ions are calculated as

$$\begin{aligned}
\Gamma^b_{e,in} &= n^b_{e,in} v^b, \\
Q^b_{e,in} &= \frac{1}{2} m_e v^b \Gamma^b_{e,in}, \\
\Gamma^b_{e,out} &= \frac{n^b}{4v^b}\left[(v^b)^2 - \frac{2e|\Delta\Phi|}{m_e}\right] \simeq \frac{1}{4} n^b v^b, \\
Q^b_{e,out} &= \frac{m_e}{8} n^b v^b \left[(v^b)^2 - \frac{2e|\Delta\Phi|}{m_e}\right] = \frac{m_e v^b}{2} \Gamma^b_{e,out}, \\
\Gamma^{th}_e &= \frac{n^{th}_e}{4}\sqrt{\frac{8kT_e}{\pi m_e}} \exp\left(\frac{e\Delta\Phi}{kT_e}\right), \\
Q^{th}_e &= (2kT_e + e|\Delta\Phi|)\Gamma_e, \\
\Gamma_i &= n_i \sqrt{\frac{kT_e}{m_i}}, \\
Q_i &= \frac{1}{2} m_i u_i^2 \Gamma_i,
\end{aligned}$$

where e is the positive unit charge, k is the Boltzmann constant, $m_{i,e}$ are the ion and electron masses, respectively, T_e is the bulk-electron temperature, $\Delta\Phi$ is the electrode or the wall potential with respect to the quasineutral plasma far from the boundaries, and $n_{i,e}$ are the ion and electron densities. Note that, according to our assumptions about the beam velocity distribution, the input beam density $n^b_{e,in}$ is usually quite different from the output beam density n^b.

In all directions relevant for ion losses, the ion velocity at the plasma-sheath boundaries may be approximately identified with the modified Bohm velocity $u_i = \alpha\sqrt{kT_e/m_i}$, where α represents a function of the plasma parameters, which is of order unity in a wide range of these parameters [10]. In the present work we use the approximation $\alpha = 1$.

The ionization cross section $\sigma_I(v)$ can be expressed as [11]

$$\sigma_I \equiv \sigma_I(e\Phi_b) = \vartheta \frac{9(e\Phi_I)^2(e\Phi_b - e\Phi_I)}{e\Phi_b(e\Phi_b + 8e\Phi_I)}, \tag{5}$$

where $e\Phi_I$ denotes the first ionization level, $e\Phi_b$ is the ionizing-electron energy and ϑ is a constant characterizing the type of gas. Our theoretical predictions and experimental explanations are based on the experimental data [12, 13] which we have used to find the constant ϑ and other relevant parameters for noble gases [8]. The ionization rate due to beam electrons can be calculated as [8]

$$\gamma^b_I = n_a \sigma_I(e\Phi^b) n^b_e v^b, \tag{6}$$

whereas the ionization rate due to thermal-electron motion can be easily obtained after making the linearization $\sigma_I \simeq \vartheta(e\Phi_b - e\Phi_I)$:

$$\gamma^{th}_I = n_a \vartheta n^{th}_e(\Phi)\sqrt{\frac{8kT_e}{\pi m_e}}(2kT_e + e\Phi_I)\exp\left(-\frac{e\Phi_I}{kT_e}\right). \tag{7}$$

We now proceed to the mathematical modeling of the discharge setup as described at the beginning of this section. In order to make the integration of Eqs (1)-(4) trivial, we assume that the plasma parameters (i.e., the plasma potential, the electron temperature, and the electron densities) may be regarded as being uniformly distributed inside the quasineutral plasma region. Thus Eq. (1) yields

$$\Gamma^b_{e,out} = \frac{I^b_{e,in}/e}{A^b_{e,out}\left[1 + \dfrac{4n_a\sigma_I V}{A^b_{e,out}}\right]}, \tag{8}$$

which for later purposes can be simply transformed into

$$I^b_{e,in} - I^b_{e,out} = \frac{I^b_{e,in}}{1 + \dfrac{A^b_{e,out}}{4n_a\sigma_I V}} = \frac{4n_a\sigma_I V}{A^b_{e,out}} I^b_{e,out}. \tag{9}$$

Evaluation of Eq. (2) leads to the relations

$$I_i = \frac{1-\mathcal{G}}{1-\mathcal{F}} 4n_a\sigma_I V \Gamma^b_{e,out} = \frac{1-\mathcal{G}}{1-\mathcal{F}}(I^b_{e,in} - I^b_{e,out}), \tag{10}$$

where the functions $\mathcal{G}$ and $\mathcal{F}$ are defined as

$$\mathcal{G} = \frac{e\Phi^b(e\Phi^b + 8e\Phi_I)}{9(e\Phi_I)^2(e\Phi^b - e\Phi_I)} \sqrt{\frac{kT_e}{2e\Phi_b}} \sqrt{\frac{8}{\pi}} (2kT_e + e\Phi_I) \exp\left(-\frac{e\Phi_I}{kT_e}\right) \tag{11}$$

and

$$\mathcal{F} = \frac{2kT_e + e\Phi_I}{e\Phi_p} \sqrt{\frac{8}{\pi}} \exp\left(-\frac{e\Phi_I}{kT_e}\right), \tag{12}$$

respectively. However, based on detailed inspection of its relevancy [8], the function $\mathcal{G}$ will be neglected for the present purposes. The quantity

$$e\Phi_p \equiv \frac{1}{n_a\vartheta \dfrac{V}{A}\sqrt{\dfrac{m_i}{m_e}}} \tag{13}$$

introduced in Eq. 12 above, is the so called "discharge efficiency". As explained in detail in accompanying paper [8] it represents the relevant similarity parameter which is of particular importance in our considerations.

Equation (10) can readily be transformed into the form

$$n_i = \frac{1}{1-\mathcal{F}} \frac{1}{1 + \dfrac{A^b_{e,out}}{4n_a\sigma_I V}} \frac{I^b_{e,in}}{eA\sqrt{kT_e/m_i}}, \tag{14}$$

which is convenient for calculating the ion density. By combining (14) with (9) and taking into account the definition of the similarity parameter Φ_p, the electron-beam density can be further expressed as

$$N \equiv \frac{n^b_e}{n_i} = \sqrt{\frac{kT_e}{2e\Phi_b}} \frac{e\Phi^b(e\Phi^b + 8e\Phi_I)}{9(e\Phi_I)^2(e\Phi^b - e\Phi_I)} (1-\mathcal{F}) e\Phi_p. \tag{15}$$

The electric-charge continuity equation (3), integrated over the plasma boundary, yields

$$I^{th}_{e,w} + I^{th}_{e,a} = I_i + I^b_{e,in} - I^b_{e,out}. \tag{16}$$

According to the definitions of the particle fluxes given above, the electron currents to the wall and the anode are $I^{th}_{e,w} = \Gamma_0(A - A_a)\exp(-\eta)$ and $I^{th}_{e,a} = \Gamma_0 A_a \exp(-\Delta\eta_a)$, where $\eta = e\Phi/kT_e$ and $\eta_a = e\Phi_a/kT_e$ are the normalized plasma and anode potentials, respectively, $\Delta\eta_a = \eta - \eta_a$ represents the anode potential drop with respect to the plasma, and $\Gamma_0 = n^{th}_e\sqrt{8kT_e/2\pi m_e}$. Consequently, the anode currents to the electrode and the wall can be correlated via the relation

$$I^{th}_{e,a} = \frac{a}{1-a}\exp(\eta_a) I^{th}_{e,w} \qquad \text{for} \quad \eta > \eta_a. \tag{17}$$

This relation holds for anode potentials which are below the plasma potential. If, however, the anode potential is above the plasma potential, we have

$$I^{th}_{e,a} = \frac{a}{1-a}\exp(\eta) I^{th}_{e,w} \qquad \text{for} \quad \eta < \eta_a. \tag{18}$$

Now Eq. (16) can be further transformed by eliminating $I^{th}_{e,a}$ with the help of the last two relations, and $I^{b}_{e,in} - I^{b}_{e,out}$ with the help of (10). The result is

$$\left[1 + \frac{a}{1-a}\exp(\eta_{(a)})\right] I^{th}_{e,w} = \left[1 + \frac{1-\mathcal{F}}{1-\mathcal{G}}\right] I_i, \tag{19}$$

where, for brevity, we have introduced the definition $\exp(\eta_{(a)}) = \exp(\eta)$ for $\eta > \eta_a$ and $\exp(\eta_{(a)}) = \exp(\eta_a)$ for $\eta < \eta_a$.

Integration of Eq. (4) over the plasma-sheath boundary yields the expression

$$kT_e(2+\eta)I^{th}_{e,w} + kT_e(2+\Delta\eta_a)I^{th}_{e,a} + \frac{1}{2}kT_eI_i = e\Phi_b(I^{b}_{e,in} - I^{b}_{e,out}) - e\Phi_I I_i, \tag{20}$$

in which the electron thermal current to the anode and the wall, as well as $I^{b}_{e,in} - I^{b}_{e,out}$, can be eliminated by using relations (17), (18), and (10), respectively. After that, the electron thermal current to the wall can be eliminated by using (19), yielding an equation in which the ion current only appears as a multiplication factor for each term. Thus relation (20) can be transformed into

$$kT_e = \frac{e\Phi_b(1-\mathcal{F}) - e\Phi_I}{1/2 + (2+\eta)(2-\mathcal{F})\dfrac{(1-a) + [1-\eta_{(a)}/(2+\eta)]a\exp(\eta_{(a)})}{1-a+a\exp(\eta_{(a)})}} \tag{21}$$

Finally, substituting in (19) the explicit expressions for the ion and electron currents to their corresponding surfaces, we obtain the two branches of solution for the plasma potential:

$$\begin{aligned} \eta_{up} &= \ln\mu\frac{1-N}{2-\mathcal{F}}\left[(1-a) + a\exp(\eta_a)\right] \\ \eta_{dn} &= \ln\mu\frac{1-N}{2-\mathcal{F}}\frac{1-a}{1-a\mu\dfrac{1-N}{2-\mathcal{F}}}, \end{aligned} \tag{22}$$

where $\mu \equiv \sqrt{m_i/2\pi m_e}$. The first solution holds for 'large' and the second for 'small' anode surfaces, i.e., for surfaces which are above or below the critical anode size

$$a_{cr} = \frac{\exp(\eta_a) - \mu\dfrac{1-N}{2-\mathcal{F}}}{\mu\dfrac{1-N}{2-\mathcal{F}}(\exp(\eta_a) - 1)}, \tag{23}$$

respectively. In order to become positive with respect to the plasma, the anode potential has to be biased above a minimum value η which equals the plasma potential in the absence of the anode:

$$\eta_a \geq \ln\mu\frac{1-N}{2-\mathcal{F}} \equiv \eta. \tag{24}$$

Obviously, this is possible only for very small anodes (probes).

Equations (14), (15), (21) and (22) represent our basic set for calculating the ion density, the beam density, the electron temperature and the plasma potential.

For an infinitely small probe, the plasma potential equals the value $\eta = \eta_{dn}$, derived in [8]. However, for a large anode ($a \to 1$) the plasma potential becomes $\eta = \eta_{up} = \eta_w + \eta_a$, showing that in this case the anode entirely takes over the role of the wall.

3 Results from the model

Figure 2 presents the electron temperature, the plasma potential, and the ion density as functions of the anode size $a = A_a/A$, as calculated from our expressions (14), (21) and (22). In Fig. 2a we show results obtained for

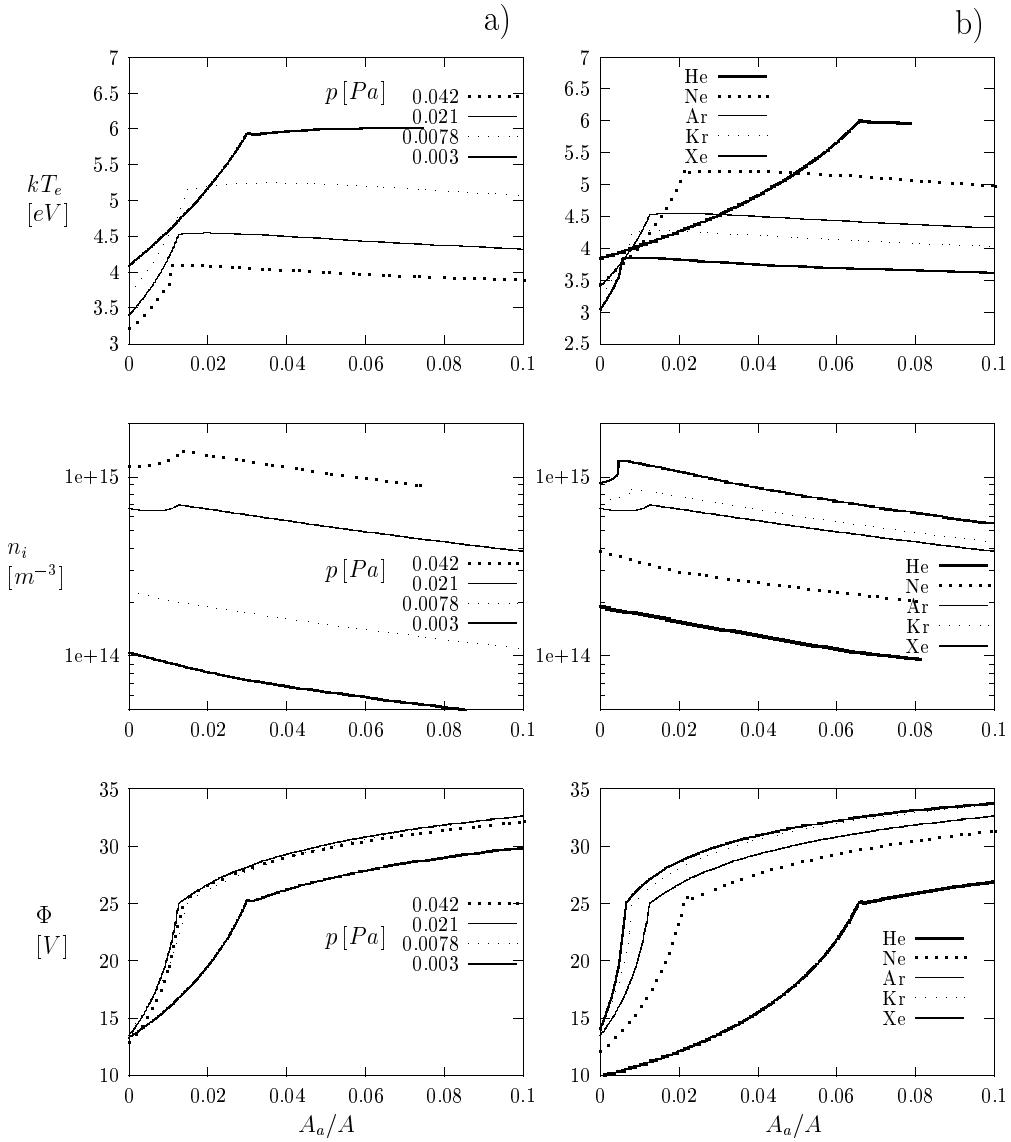

Fig. 2 Theoretically determined electron temperature, ion density and plasma potential as functions of the anode size: (a) for various pressures in Ar, (b) at a constant pressure for different gases. The anode potential is $\Phi_a = 25\,V$ in both cases (a) and (b).

an argon discharge with variable gas pressure, whereas in Fig. 2b we present the results obtained at the constant pressure p = 0.04 Pa for different types of gases. The numerical values of the external parameters have been chosen so as to be as close as possible to a realistic experimental situation. Thus we have limited the presentation of the functional dependence to the range from $a = 0$ to $a = 0.1$. The limit $a \to 1$ leads to a discharge without magnetic confinement in which the anode plays the role of a new wall.

The effective reference dimension of the system is $V/A_w \simeq 0.068\,\mathrm{m}$. The effective total area for primary-electron losses, in the case of an infinitely small anode, is $A^b_{e,out} = 0.1A_w$. It has been estimated that this value reproduces well the effects of the magnetic cusps on primary-electron confinement in the Innsbruck DP device. Additional parameters are the beam energy $e\Phi^b = 60\,\mathrm{eV}$, the anode potential $\Phi_a = 25\,\mathrm{V}$, and the discharge current $I_d \equiv I^b_e = 0.5\,\mathrm{A}$.

From Fig. 2a we see that the electron temperature is rather sensitive to change in the size of a positively biased anode, whereas the plasma potential is entirely determined by the anode size. For a typical range of laboratory pressures (in which experiments in DP machines are most frequently reported), represented by the three highest values in the figure, the plasma potential is practically independent of the pressure. A common feature is that the plasma potential becomes higher than the applied anode potential for an anode size $A_a/A \simeq A_a/A_w \simeq 2/\mu$. For our experimental chamber, where A_w is approximately 0.5 m^2, this yields $A_{a,cr} \simeq 100\,\mathrm{cm}^2$. However, deviations from this crude estimate are obvious for both high and low pressures, since in the first case there is an influence of thermal ionization (function $\mathcal{F}$), whereas in the second case the effects of beam electrons prevail (factor $1 - N$).

Unlike the experimental results in [3], our model predicts an increase in electron temperature with increasing anode surface area. This electron "heating" saturates near the critical anode size for which the plasma potential reaches the anode potential. The electron temperature again decreases with increasing anode surface. In addition, there are no significant changes in plasma density with varying anode size. The density decreases monotonically with increasing anode size, provided that the pressure is sufficiently low. For high pressures, however, a non-monotonic behavior is observed.

As emerges from Fig. 2b, the global behavior of the plasma parameters in lighter gases resembles the behavior in Fig. 2a of the plasma parameters for argon approaching smaller pressures. This is an indication that the similarity rule with respect to the gas pressure and type holds both in the presence and in the absence of an anode. A remarkable feature of Fig 2b is that a clear distinction between the different gases can be made by just looking at the critical anode size for which the plasma potential equals the anode potential.

4 Experimental results

Our experiments were performed in a setup as shown schematically in Fig 3. It was made suitable for measuring plasma parameters as functions of the anode surface area by installing two one-sided plane-parallel electrodes, the non-insulated sides of which fitted on one another with the possibility to increase their total surface areas from zero to 488 cm^2 by shifting one of the electrodes, cf. Fig 3. As in the experiments presented in the accompanying

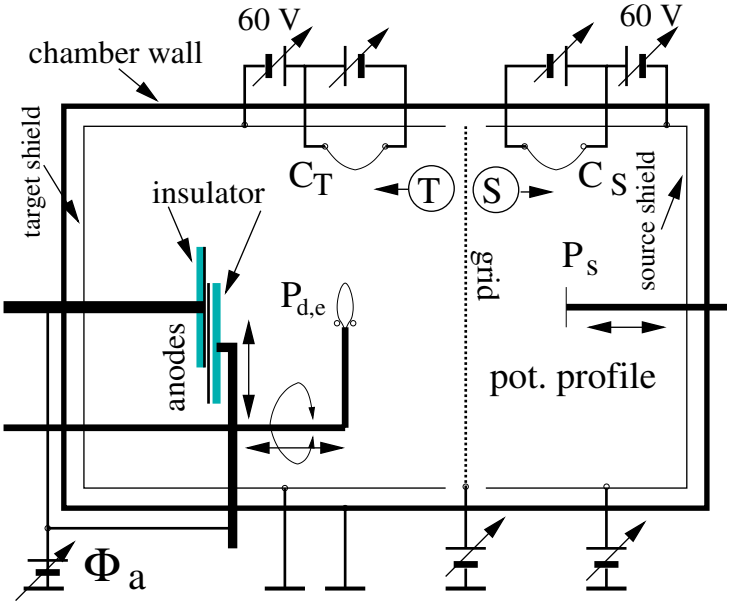

Fig. 3 Experimental set-up of the Innsbruck double-plasma device for measuring the dependence of the plasma parameters on the biased anode size. The hot filament 'cathodes' are denoted as C_T and C_S. The source (S) and target (T) chambers are shielded from the wall and may be biased at arbitrary potentials. Ionizing electrons of approximate $e\Phi^b \simeq 60\,\mathrm{eV}$ are extracted by the target chamber from the source region. The plasma parameters are measured by movable emissive and double-plane probes (P_d, P_s) The anode of variable size is realized by using two plane-parallel electrodes with active surfaces fitting each other at variable extent

paper [8], most of the measurements were performed in the target chamber, in which the discharge was maintained by drawing the ionizing electrons from the source plasma chamber. The reference value of the ionizing beam electron energy had to be re-adjusted after any increase in the plasma potential in the source chamber, in order to maintain a constant value (-60 V). This was achieved by adjusting the biasing potential of the separating mesh-grid - anode-screen system of the source chamber. However, changing the beam electron energy has no serious effects on the measured results since the plasma potential and the bulk-electron temperature are not sensitive to this parameter in a wide range of its experimental values. The discharge current in the source chamber was held constant, so that the source plasma density and, consequently, extracted beam current was as close as possible to 0.5 A.

The plasma parameters in the target chamber were measured by a diagnostic system $P_{d,e}$ consisting of a double plane Langmuir probe and an emissive probe mounted on the same shaft, enabling radial and axial scanning. The diagnostics of the source chamber consisted of a single one-sided plane probe P_s movable only in the axial direction. To check the theoretical results for the plasma potential in the source chamber, this probe had to be replaced with an emissive probe.

Our main experimental results are presented in Fig. 4a, where we present the dependence on the anode size of our experimental electron temperature, plasma density and plasma potential in argon. This figure has to be compared with the corresponding theoretical one presented in Fig. 2a. The data were usually taken by changing the anode surface in steps of 12 cm^2.

There are several important features that need to be pointed out. First, it is clear that the electron temperatures and plasma potentials presented in Fig. 4a are well below those predicted by the theory, but are still comparable. The source of discrepancy could probably be removed by modifying our basic formulas so as to include the total inelastic gas cross-section. On the other hand, Fig 4a shows that the experimental dependence of the electron temperature on the anode size is even much stronger than predicted by the theory. Thus, the model *underestimates* the electron "heating" due to the presence of an electron-absorbing boundary, but the reason is not quite clear. Again, a possibility to overcome this problem would be the inclusion of the volume energy losses, which are more efficient provided the thermal electron population is better confined. The next feature is related to the predicted dependence on the pressure, in comparison with the experimental results in Fig. 4a. In the model we have to decrease the pressure by a factor of approximately 15 in order to increase the critical anode surface by a factor of two, whereas in the experiments an increase in critical anode surface by a factor of three was observed by changing the pressure by a factor of only five. This is because all our calculations require exact knowledge of the similarity parameter which, on the other hand, depends on an experimentally rather uncertain quantity V/A evaluated by ignoring many details such as, e.g. mechanical supports. The experimental critical anode size a_{cr} for the two higher values of the argon pressure lies between 0.16 and 0.20, in agreement with the theoretical reference value in the absence of high- and low-pressure effects. The corresponding theoretical values are obviously shifted to the left, indicating underestimation of the theoretical pressure or, equivalently, the effective dimension V/A, whose actual value may lie well below our theoretical one (0.068).

In Fig. 4b we show the measured dependencies of the plasma parameters on the anode size for He, Ne, Ar, Kr and Xe. These results have to be compared with the corresponding theoretical predictions given in Fig 2b. The predicted behavior of the plasma parameters as functions of the anode size seems to be well confirmed qualitatively. The critical anode size for all gases turns out to be underestimated except in the case of He, but the global behavior is quite correct. In addition, in contrast with the previous case, we here observe indications that the plasma density may indeed be a non-monotonic function of the anode size.

5 Discussion

Our results may be applied to understanding many particular phenomena related to electron-absorbing boundaries in plasmas. As a particularly important application we here mention the very general problem of an anode-type double layer [5]. This apparently simple phenomenon occurs under rather special conditions, i.e., at relatively high pressures and sufficiently small anode sizes. To answer the question regarding the critical gas pressure above which a double layer can be formed we apply our relations (9) and (10) to a plasma confined by a double layer and maintained by the beam electrons, which acquire the main part of their kinetic energy in the region of the double layer. After simple rearrangements and ignoring ionization processes due to thermal motion we obtain

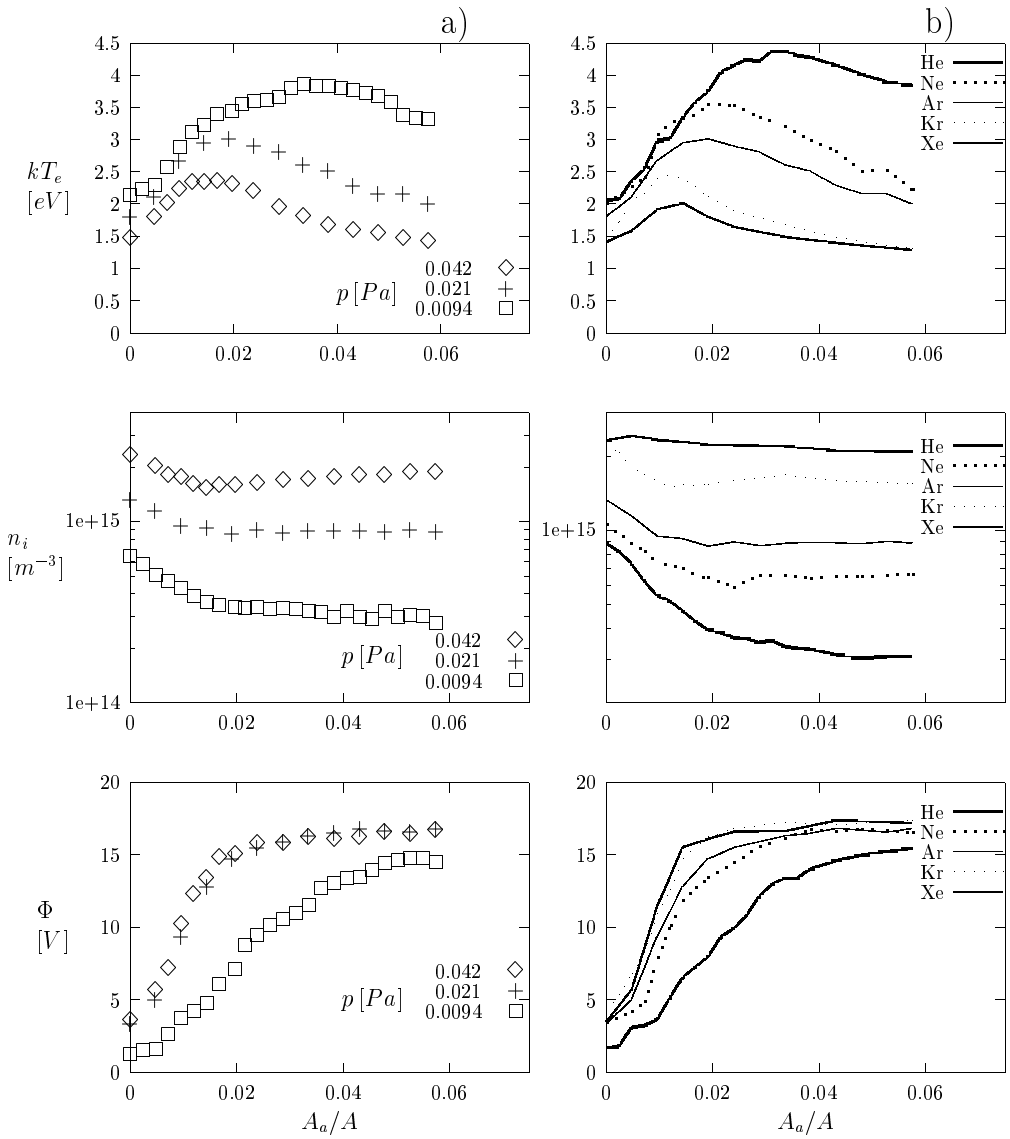

Fig. 4 Experimentally measured electron temperature, ion density and plasma potential as functions of the anode size: (a) for various pressures in Ar, (b) at a constant pressure for different gases. The anode potential is $\Phi_a = 15\,\mathrm{V}$ in both cases

$\Gamma_i \simeq \Gamma^b_{e,in}/(1 + A_{dl}/4n_a\sigma_I V_{dl})$, where Γ_i is the ion outflux from the plasma confined by the double layer and $\Gamma^b_{e,in}$ originates from the thermal electrons at the low-potential side of the double layer. Combining this relation with the simplest approximation of the Langmuir condition, $\Gamma_i \simeq \Gamma^b_{e,in}\sqrt{m_e/m_i}$ (for a more exact result see [14]), and using the definition of the similarity parameter Φ_r, we obtain the result

$$\Phi_p = \frac{36(e\Phi_I)^2(e\Phi_{dl} - e\Phi_I)}{e\Phi_{dl}(e\Phi_{dl} + 8e\Phi_I)}. \tag{25}$$

Since this expression holds for $\Phi_{dl} > \Phi_I$ and, moreover, the right-hand side has a maximum for $\Phi_{dl} = 4\Phi_I$, we obtain the condition

$$0 < \frac{\Phi_p}{\Phi_I} < \frac{9}{4}, \tag{26}$$

which represents an elementary but rather general estimate of the maximum discharge efficiency for which a double layer can still exist.

For relatively large plasma systems, such as the Innsbruck DP device (V/A=0.068 cm), application of the condition (26) to argon yields a minimum chamber pressure of roughly 0.003 Pa (as read at the Penning gauge) above which the plasma can still be maintained. According to our estimates, the effective dimension of an eventually formed additional plasma confined by a double-layer surface should at least be fifty times smaller. Consequently, a double layer may exist provided the argon pressure is well above 0.15 Pa.

Thus, summarizing our example we conclude that in our DP device an anode-type double layer can be formed if we use electrodes smaller than 0.8 cm in diameter and rise the argon pressure above 0.15 Pa. Smaller anodes (i.e., probes) obviously require higher pressures. With regard to more general cases, however, we must not forget that the relevant external parameter is neither the pressure nor the double-layer dimension, but rather a product of these quantities with the square root of the mass ratio and the constant ϑ. Therefore, in order to extend the range of pressures in which a double layer can still persist toward low pressures, we have to use heavier gases. The use of lighter gases, on the other hand, requires pressures so high that both the theory and diffusion pumps normally fail.

6 Conclusion

We have investigated the plasma parameters in a DP device, in the presence of a positively biased electrode. A model has been developed which predicts the behavior of the plasma parameters for an electron-absorbing electrode surface of variable size The theoretical results have been confirmed by measurements of plasma parameters in appropriate conditions. It has been predicted by our model and furthermore found experimentally that an electrode, biased positively with respect to the wall potential, can significantly increase not only the plasma potential as previously reported [3], but also the electron temperature.

It has been found that the plasma potential becomes higher than the applied anode potential (positive with respect to the wall) for an anode size which is approximately $2/\mu$ times the total plasma surface. Anodes with sizes above this value dominate thermal electron losses over the wall. Consequently, the overall particle balance becomes determined by a large anode, which thus takes the role of the new main wall for plasma. Quantitatively speaking, "large" means just greater than $2/\mu$.

Consequences for experiments with anode-type double layers have been discussed in the light of the results presented. General approximate conditions for the existence of anode-type double layers have been described and applied to the Innsbruck DP machine. These conditions correlate external parameters with each other, e.g., the chamber dimension with the anode parameters and the anode diameter with the gas pressure and type. In addition, our results show that, in the presence of an anode-type double layer, the plasma parameters at both of its sides are appreciably influenced and even determined by the presence of the double layer itself.

Acknowledgements The authors would like to thank Prof. A. Piel for many valuable comments and suggestions. This work was supported by the Fonds zur Förderung der wissenschaftlichen Forschung (Austria) under grant Nos. P8709, P8405 and P15013.

References

[1] Y. Nakamura, Y. Nomura, Phys. Lett. **65A**, 415 (1978)
[2] R.B. Spielman, J.S. DeGroot, D.A. Rasmussen, J. Appl. Phys. **47**, 1909 (1976)
[3] K.R. MacKenzie, R.J. Taylor, D. Kohn, E. Ault, H. Ikezi, Appl. Phys. Lett. **18**, 529 (1971)
[4] M.-H. Cho, N.C. Hershkowitz, T. Intrator, J. Appl. Phys. **67**, 3254 (1990)
[5] I.R. Langmuir, Phys. Rev. **33**, 954 (1929)
[6] H. Amemiya, Y. Nakamura, Plasma Phys. **26**, 1613 (1986)
[7] B. Song B, N. D'Angelo, R.L. Merlino, J. Phys. D **24**, 1789 (1991)
[8] N. Jelić, S. Kuhn, R. Schrittwieser, submitted to Contrib. Plasma Phys. (2002)
[9] K.N. Leung, N. Hershkowitz, K.R. MacKenzie, Phys. Fluids **19**, 1045 (1976)
[10] N. Jelić, M. Čerček, M. Stanojević, T. Gyergyek, J. Phys. D **27**, 2487 (1994)
[11] W.E. Golant, A.P. Zhilinskiy, I.E. Saharov, *Osnovi Fiziki Plazmi*, Atomizdat, Moskow (1997)
[12] K. Stefan, H. Helm, T.D. Märk, J. Chem. Phys. **73**, 3763 (1980)
[13] K. Stefan, T.D. Märk, J. Chem. Phys. **82**, 31 (1984)
[14] N. Jelić, M. Čerček, M. Stanojević, T. Gyergyek, J. Plasma Phys. **51**, 233 (1994)